High-field magnetization of $SrMn_3P_4O_{14}$ exhibiting a quantum-mechanical magnetization plateau and classical magnetic long-range order

Masashi Hase,[1,*] Tao Yang,[2,3] Rihong Cong,[2] Jianhua Lin,[2] Akira Matsuo,[4] Koichi Kindo,[4] Kiyoshi Ozawa,[1] and Hideaki Kitazawa[1]

[1]*National Institute for Materials Science (NIMS), 1-2-1 Sengen, Tsukuba, Ibaraki 305-0047, Japan*

[2]*College of Chemistry and Molecular Engineering, Peking University, Beijing 100871, People's Republic of China*

[3]*Department of Chemistry and Chemical Biology, Rutgers, The State University of New Jersey, Piscataway, New Jersey 08854, USA*

[4]*The Institute for Solid State Physics (ISSP), The University of Tokyo, Kashiwa, Chiba 277-8581, Japan*

(Received 18 June 2009; revised manuscript received 1 July 2009; published 5 August 2009)

It has not been investigated adequately whether a quantum-mechanical nature can persist in a classical magnetic long-range order in systems with large spins. The recent experimental study reports a quantum-mechanical 1/3 magnetization plateau at greater than 2 T and a classical canted antiferromagnetic long-range order in weak magnetic fields in $SrMn_3P_4O_{14}$ possessing spin 5/2 [Yang *et al.*, Inorg. Chem. **47**, 2562 (2008)]. The origins of the plateau are quantum-mechanical discrete energy levels of magnetic eigenstates. Although the spin system of $SrMn_3P_4O_{14}$ is inferred to be a trimerized spin chain, the magnetism has not been explained quantitatively. We have conducted high-field magnetization measurements of $SrMn_3P_4O_{14}$ powders and determined that the spin system is a spin-5/2 trimer with weak three-dimensional intertrimer interactions. This spin system can account for the magnetization plateau and magnetic long-range order.

DOI: 10.1103/PhysRevB.80.054402 PACS number(s): 75.45.+j, 75.10.Jm, 75.60.Ej, 75.40.Cx

I. INTRODUCTION

We infer effective Hamiltonians from crystal structures when we study magnetism of substances. Effective Hamiltonians are described using quantum spin operators. Physical quantities are calculated quantum mechanically from effective Hamiltonians and are compared with experimental results. Meanwhile, we usually treat spins as vectors (classical spins) and consider arrangements of vectors in magnetic long-range order (LRO). These arrangements are often not eigenstates of inferred Hamiltonians. Consequently, properties of magnetic LRO cannot be understood fully within frameworks of classical models in low-dimensional systems formed by small spins. Quantum-mechanical nature remains. For example, in spin-gap systems with spin 1/2 such as the spin-Peierls system in $CuGeO_3$ (Ref. 1 and 2) and the two-leg ladder system in $SrCu_2O_3$ (Ref. 3 and 4) doped with impurities,[5–9] antiferromagnetic LRO (AF-LRO) appears. Nonetheless we have observed an excitation corresponding to a singlet-triple gap in pure systems.[10]

It has not been studied adequately whether the quantum-mechanical nature can remain in classical magnetic LRO in systems with large spins. Recently, some of the authors present newly synthesized compounds $AMn_3P_4O_{14}$ (A=Sr and Ba) and observed a quantum-mechanical 1/3 magnetization plateau at greater than 2 T and a classical magnetic LRO in weak magnetic fields.[11] Only Mn^{2+} ions ($3d^5$) have localized spin 5/2. Magnetic LRO appears below transition temperature T_c=2.6 K. It is expected that spin-5/2 trimerized chains with a J_1-J_1-J_2 interaction pattern exist. Both J_1 and J_2 are exchange-interaction parameters (Fig. 1). Before the report of the magnetization plateau in $AMn_3P_4O_{14}$ (A=Sr and Ba),[11] a magnetization plateau in trimerized chains has been observed experimentally only in $Cu_3(P_2O_6OH)_2$ (spin 1/2).[12,13] Assuming that the J_1 and J_2 interactions are antiferromagnetic and ferromagnetic (F), respectively, we can understand the magnetism of $AMn_3P_4O_{14}$ (A=Sr and Ba) qualitatively as follows. Each chain has a finite magnetic moment below T_c. AF-LRO with (without) spontaneous magnetization appears in $SrMn_3P_4O_{14}$ ($BaMn_3P_4O_{14}$) caused by imperfect (perfect) cancellation of finite magnetic moments of chains. Isostructural compounds $ANi_3P_4O_{14}$ (A=Ca, Sr, Ba, and Pb) (Ref. 14) and $ACo_3P_4O_{14}$ (A=Sr and Ba) (Ref. 11) exhibit similar AF-LRO with spontaneous magnetization (canted AF-LRO) but not a 1/3 magnetization plateau. A tendency for the plateau is seen above T_c in $AMn_3P_4O_{14}$ (A=Sr and Ba). Accordingly, the 1/3 magnetization plateau is not caused by magnetic LRO. The origins of the plateau are quantum-mechanical discrete energy levels of magnetic eigenstates. The quantum-mechanical nature can remain even in classical magnetic LRO in systems with large spins (5/2).

Trimerized chains do not necessarily exhibit 1/3 magnetization plateaus. We must clearly show the origins of the 1/3 magnetization plateau in $SrMn_3P_4O_{14}$. We need to determine the spin system more quantitatively. We must also discuss whether magnetic LRO is possible. Magnetization curves

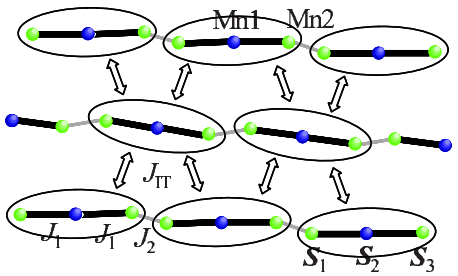

FIG. 1. (Color online) The spin system in $SrMn_3P_4O_{14}$. Two crystallographic Mn^{2+} sites (Mn1 and Mn2) exist. They possess spin 5/2. We consider J_1, J_2, and J_{IT} (intertrimer) interactions to explain magnetism of $SrMn_3P_4O_{14}$. Ellipses indicate trimers whose spin operators are S_1, S_2, and S_3.

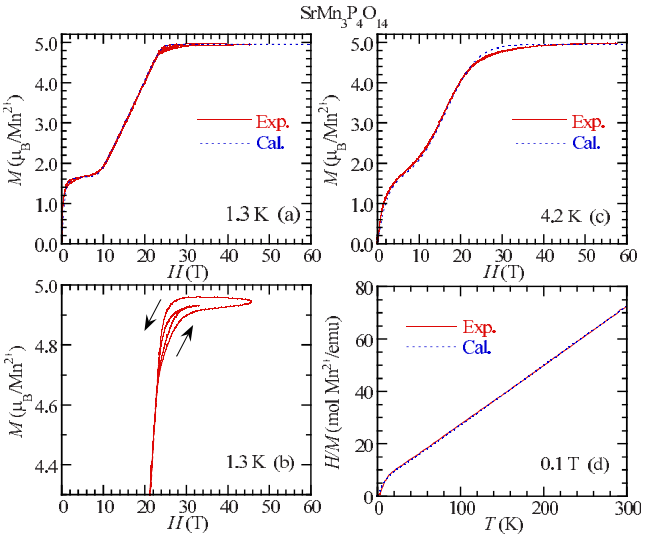

FIG. 2. (Color online) (a) Magnetization curves of $SrMn_3P_4O_{14}$ (red solid lines) and the calculated magnetization curve of the spin-5/2 trimer with $J_1=4.0$ K at 1.3 K (blue dashed line). μ_B is the Bohr magneton. (b) Magnetization curves of $SrMn_3P_4O_{14}$ at 1.3 K around 26 T. Arrows indicate directions of magnetic field scans. (c) Magnetization curves of $SrMn_3P_4O_{14}$ (red solid lines) and the calculated magnetization curve of the spin-5/2 trimer with $J_1=4.0$ K at 4.2 K (blue dashed line). (d) Temperature dependence of H/M in 0.1 T of $SrMn_3P_4O_{14}$ (red solid line) and that of the inverse of the calculated susceptibility in the spin-5/2 trimer with $J_1=4.0$ K (blue dashed line).

have been obtained only less than 5 T. Therefore, we cannot determine the spin system correctly. Consequently, we have investigated $SrMn_3P_4O_{14}$ using high-field magnetization measurements.

II. METHODS OF EXPERIMENTS

Single crystals of $SrMn_3P_4O_{14}$ have been synthesized under hydrothermal conditions at 200 °C. Details of the synthesis have been reported in Ref. 11. Each crystal was small. Therefore, we used pulverized crystals for magnetization measurements. High-field magnetization measurements were conducted using an induction method with a multilayer pulsed field magnet installed at the Institute for Solid State Physics, the University of Tokyo. Magnetization data were collected at 1.3 and 4.2 K in magnetic fields up to $H=58$ T. We measured magnetization up to $H=5$ T using a superconducting quantum interference device (SQUID) magnetometer (MPMS-5S; Quantum Design).

III. RESULTS AND DISCUSSION

Figure 2(a) portrays magnetization M curves of $SrMn_3P_4O_{14}$ at 1.3 K (red solid line). The 1/3 magnetization plateau exists between 2 and 10 T. The magnetization is saturated at greater than 24 T. A value of the saturated magnetization is 4.95 μ_B, which means that a powder-average g value is 1.98. A powder-average g value has been evaluated independently as 1.95 from temperature T dependence of M/H greater than 30 K.[11] Both the g values are very close to each other. A value of a spin-orbit interaction in $3d^5$ is small. Therefore, it is expected that a g value of $3d^5$ spin 5/2 is almost equal to 2. This expectation is consistent with the experimental results. At around 26 and 2 T, hysteresis is apparent between magnetization curves measured in increasing and decreasing fields. Figure 2(b) depicts an enlarged image of the experimental magnetization curves around 26 T. The duration of the magnetic fields is constant. Therefore, the sweep rate decreases in a decrease in the maximum field. Hysteresis of around 26 T is less apparent when the sweep rate is smaller. Hysteresis of around 2 T does not exist in magnetization curves measured in static fields using a SQUID magnetometer. The hysteresis is more apparent at lower temperatures. Consequently, we have concluded that the hysteresis of magnetization is attributable to magnetocaloric effects. Figure 2(c) presents magnetization curves at 4.2 K (red solid line). The 1/3 magnetization is less apparent and the magnetization rounds at around 26 T. A red solid line in Fig. 2(d) indicates H/M of $SrMn_3P_4O_{14}$ in 0.1 T. The experimental H/M is linearly proportional to T greater than 20 K and rapidly decreases at temperatures less than 20 K. The experimental H/M agrees with that reported in Ref. 11.

We consider an effective Hamiltonian that can account for magnetism of $SrMn_3P_4O_{14}$. Probably, spin 5/2 on Mn^{2+} ions is a Heisenberg spin because an electron configuration is $3d^5$. The experimental result that the powder-average g value 1.98 in $SrMn_3P_4O_{14}$ is close to 2 does not contradict Heisenberg spins. The Mn1 and Mn2 atoms are both coordinated octahedrally by six oxygen atoms. Symmetries of crystal fields affecting the Mn^{2+} ions are nearly cubic. It is inferred that single-ion anisotropy of the Mn^{2+} ions is small. Small single-ion anisotropy is consistent with the small spin-flop field (0.07 T).[11]

Main interactions between spins are exchange interactions. We consider only the AF J_1 interaction as a first approximation because it is inferred that the magnitude of the J_1 interaction is larger than that of the J_2 interaction.[11] The J_1 interactions form spin-5/2 trimers as shown in Fig. 1. The effective Hamiltonian of the trimer is written as

$$\mathcal{H} = J_1(S_1S_2 + S_2S_3). \tag{1}$$

As shown later, magnetization curves and magnetic susceptibility calculated from this Hamiltonian can reproduce experimental results well.

We have calculated all eigenenergies using an exact diagonalization method. Table I presents the eigenenergies. We evaluated H dependence of magnetization M and T dependence of magnetic susceptibility χ using the following equations:

$$M = \frac{g\sum_{E}\sum_{S_z^T=-S^T}^{S^T} S_z^T \exp\left(-\frac{E-g\mu_B HS_z^T}{k_BT}\right)}{\sum_{E}\sum_{S_z^T=-S^T}^{S^T} \exp\left(-\frac{E-g\mu_B HS_z^T}{k_BT}\right)}, \tag{2}$$

TABLE I. Eigenenergies and their total spins in the spin-5/2 trimer.

S^T	E/J_1					
15/2	12.5 ($E15_1$)					
13/2	5 ($E13_1$)	10 ($E13_2$)				
11/2	−1.5 ($E11_1$)	3.5 ($E11_2$)	7.5 ($E11_3$)			
9/2	−7 ($E09_1$)	−2 ($E09_2$)	2 ($E09_3$)	5 ($E09_4$)		
7/2	−11.5 ($E07_1$)	−6.5 ($E07_2$)	−2.5 ($E07_3$)	0.5 ($E07_4$)	2.5 ($E07_5$)	
5/2	−15 ($E05_1$)	−10 ($E05_2$)	−6 ($E05_3$)	−3 ($E05_4$)	−1 ($E05_5$)	0 ($E05_6$)
3/2	−12.5 ($E03_1$)	−8.5 ($E03_2$)	−5.5 ($E03_3$)	−3.5 ($E03_4$)		
1/2	−10 ($E01_1$)	−7 ($E01_2$)				

$$\chi = \frac{g^2\mu_B^2}{3k_BT}\frac{N_A}{3}\frac{\sum_E S^T(S^T+1)(2S^T+1)\exp\left(-\frac{E}{k_BT}\right)}{\sum_E (2S^T+1)\exp\left(-\frac{E}{k_BT}\right)}. \quad (3)$$

The summation Σ_E is performed for the eigenenergies presented in Table I. Parameters S^T and S_z^T, respectively, signify a total spin of eigenstates and a z component of the total spin. In addition, μ_B, N_A, and k_B, respectively, signify the Bohr magneton, Avogadro's number, and Boltzmann constant. We first compared the experimental magnetization curves at 1.3 K with calculated ones at 1.3 K with various values of J_1 because magnetic fields of the plateau and the saturation are apparent. A calculated curve with $J_1=4.0$ K (blue dashed line) best fits the experimental curves as shown in Fig. 2(a). Consistency between the experimental and calculated curves is slightly worse when $J_1=3.8$ or 4.2 K (not shown). We have evaluated that $J_1=4.0\pm0.1$ K. A calculated magnetization curve with $J_1=4.0$ at 4.2 K can well reproduce the experimental curves at 4.2 K. We also calculated magnetization curves with various values of J_1 at 4.2 K. We cannot find another value of J_1 with which a calculated curve can explain the experimental curves better. Temperature dependence of the inverse of calculated magnetic susceptibility with $J_1=4.0$ K is consistent with that of the experimental susceptibility. The calculated magnetic susceptibility includes small constant susceptibility 2×10^{-4} emu/mol Mn^{2+}. The main origin of constant susceptibility is Van Vleck paramagnetism. Therefore, the value of the constant susceptibility seems reasonable. The Weiss temperature θ has been calculated as 23.3 K from $J_1=4.0$ K using a formula $\theta=2S(S+1)J_1/3$. The Weiss temperature was evaluated independently as 22.3 K from the temperature dependence of susceptibility greater than 30 K using the Curie-Weiss law. The two θ values are very similar.

In the previous paragraph, we described a comparison of the experimental results with those calculated for the spin-5/2 AF trimers. Strictly speaking, we should compare the experimental results with calculated ones of spin-5/2 trimerized chains with the J_1-J_1-J_2 interaction pattern. Magnetization and magnetic susceptibility, however, are not calculated in spin-5/2 trimerized chains. As described below, nonnegligible ferromagnetic J_2 interactions, which were considered in $SrMn_3P_4O_{14}$, are expected to generate differences between the experimental and calculated results of magnetization and magnetic susceptibility. Gu *et al.*, calculated magnetization of trimerized chains using the density-matrix renormalization-group method.[15] The spin value is 1/2, 1, 3/2, or 2. When the J_1 and J_2 interactions are AF and F, respectively, the value of the saturation field depends only on that of the AF J_1 interaction in all the spin values. An identical result is expected for spin 5/2. We must obtain that the value of J_1 is close to 4.0 K if we compare the experimental magnetizations with calculated ones of spin-5/2 trimerized chains in the vicinity of the saturation field. Magnetic susceptibility with $J_1=4.0$ K and $J_2=0$ K (AF trimer) must differ from that with $J_1=4.0$ K and non-negligible values of J_2. The AF trimer with $J_1=4.0$ K can explain the experimental results quantitatively. We expect that trimerized chains cannot account for the experimental results.

The results described above demonstrate that the AF J_1 interaction is dominant. Magnetic LRO appears at low T. Therefore, weak three-dimensional intertrimer interactions also exist. The spin system determined in the present study is presented in Fig. 1. We do not know which magnitude is the larger of J_2 and J_{IT}. It is actually impossible to calculate magnetization curves and susceptibility considering J_1, J_2, and J_{IT}. We cannot estimate values of the J_2 and J_{IT} interactions. The spin system and magnetism of $SrMn_3P_4O_{14}$ are similar to those of $A_3Cu_3(PO_4)_4$ (A=Ca, Sr, and Pb). These cuprates have one-dimensional arrays of spin-1/2 trimers and show a 1/3 magnetization plateau and magnetic LRO.[16–18]

The origins of the 1/3 magnetization plateau are quantum-mechanical discrete energy levels of magnetic eigenstates in the spin-5/2 trimer. The discrete energy levels remain in spite of the introduction of weak three-dimensional intertrimer interactions. The ground states (GSs) of the trimer in the zero magnetic field are the $E05_1$ states in Table I and Fig. 3. The $E05_1$ states are sixfolded degenerate ($S_z^T=\pm5/2$, $\pm3/2$, and $\pm1/2$). The trimer can have a finite magnetic moment. Therefore, the magnetic LRO is stabilized by the J_1 and weak three-dimensional intertrimer interactions.[19] The canted AF-LRO results from imperfect cancellation of the finite magnetic moments of the trimers. Although we infer that intertrimer interactions are weak, T_c/J_1 is 0.65. The large value of the Mn^{2+} spin (5/2) might provide the relative high T_c. In Ref. 11, it is inferred that origins of the 1/3 magnetization plateau are good one-dimensional characteristics and strong AF intrachain interactions. This inference is

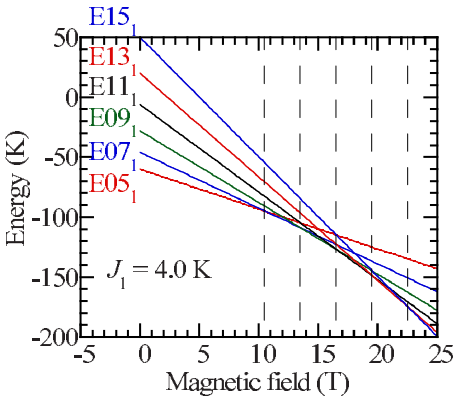

FIG. 3. (Color online) Magnetic field dependence of some eigenenergies in the spin-5/2 trimer with $J_1=4.0$ K. We show energies in cases where $S_z^T=S^T$. Vertical dashed lines represent transition fields of Ei_1 to $Ei+1_1$.

practically correct. Strictly speaking, cluster (trimer) characteristics are intrinsic. Considering similarity between $SrMn_3P_4O_{14}$ and $BaMn_3P_4O_{14}$, probably, we can explain the magnetism of $BaMn_3P_4O_{14}$ using a spin-5/2 trimer model.

We can explain the magnetization curves at low T based on ground states of the trimers in magnetic fields. In weak magnetic fields, one of the six $E05_1$ states that has $S_z^T=5/2$ is GS. The magnetic moment of the $E05_1$ state with $S_z^T=5/2$ is saturated around 2 T and the 1/3 magnetization plateau appears. In other words, the canted AF-LRO can be easily destroyed by application of magnetic fields. The magnetic moments ($S_z^T=5/2$) of trimers tend to a forced ferromagnetic alignment. The plateau remains until 10.6 T because of the energy difference between the $E05_1$ state and the $E07_1$ state with $S^T=S_z^T=7/2$. The ground state moves sequentially to the $E09_1$ state with $S^T=S_z^T=9/2$ in 13.6 T, to the $E11_1$ state with $S^T=S_z^T=11/2$ in 16.6 T, to the $E13_1$ state with $S^T=S_z^T=13/2$ in 19.6 T, and to the $E15_1$ state with $S^T=S_z^T=15/2$ in 22.6 T. At 0 K, four other magnetization plateaus exist. The width of these plateaus is only 3 T. At finite temperatures, these plateaus are not observable. The magnetization increases gradually until the saturation field. In future studies, it is necessary to investigate magnetic excitations using inelastic neutron-scattering measurements. We will observe magnetic excitations at differences between the eigenenergies presented in Table I. It is important to determine the magnetic structure using neutron-diffraction measurements. We will be able to confirm signs of J_1 and J_2.

IV. CONCLUSIONS

We have performed high-field magnetization measurements of $SrMn_3P_4O_{14}$ powders. Magnetization curves at 1.3 K exhibit the quantum-mechanical 1/3 magnetization plateau between 2 and 10 T, and saturation at greater than 24 T. Magnetization curves and magnetic susceptibility calculated for the spin-5/2 trimer with interaction value of 4.0 K are consistent with experimental results. The spin system in $SrMn_3P_4O_{14}$ can be regarded as the trimer with weak three-dimensional intertrimer interactions. The origins of the 1/3 magnetization plateau are quantum-mechanical discrete energy levels of magnetic eigenstates in the spin-5/2 trimer. The discrete energy levels remain in spite of the addition of intertrimer interactions. Each trimer has a finite magnetic moment. Therefore, the magnetic long-range order is stabilized by the intratrimer interaction and weak three-dimensional intertrimer interactions.

ACKNOWLEDGMENTS

We are grateful to M. Kohno for invaluable discussion. This work was partially conducted under the Visiting Researcher's Program of the Institute for Solid State Physics, the University of Tokyo. This work was partially supported by grants from NIMS and by a Grant-in-Aid for Scientific Research on priority Areas High Field Spin Science in 100T (No.451) from the Ministry of Education, Culture, Sports, Science, and Technology (MEXT).

*hase.masashi@nims.go.jp

[1] M. Hase, I. Terasaki, and K. Uchinokura, Phys. Rev. Lett. **70**, 3651 (1993).
[2] M. Hase, I. Terasaki, K. Uchinokura, M. Tokunaga, N. Miura, and H. Obara, Phys. Rev. B **48**, 9616 (1993).
[3] E. Dagotto, J. Riera, and D. Scalapino, Phys. Rev. B **45**, 5744 (1992).
[4] M. Azuma, Z. Hiroi, M. Takano, K. Ishida, and Y. Kitaoka, Phys. Rev. Lett. **73**, 3463 (1994).
[5] M. Hase, I. Terasaki, Y. Sasago, K. Uchinokura, and H. Obara, Phys. Rev. Lett. **71**, 4059 (1993).
[6] M. Hase, N. Koide, K. Manabe, Y. Sasago, K. Uchinokura, and A. Sawa, Physica B **215**, 164 (1995).
[7] M. Hase, K. Uchinokura, R. J. Birgeneau, K. Hirota, and G. Shirane, J. Phys. Soc. Jpn. **65**, 1392 (1996).
[8] M. Azuma, Y. Fujishiro, M. Takano, M. Nohara, and H. Takagi, Phys. Rev. B **55**, R8658 (1997).
[9] M. Azuma, M. Takano, and R. S. Eccleston, J. Phys. Soc. Jpn. **67**, 740 (1998).
[10] M. C. Martin, M. Hase, K. Hirota, G. Shirane, Y. Sasago, N. Koide, and K. Uchinokura, Phys. Rev. B **56**, 3173 (1997).
[11] T. Yang, Y. Zhang, S. Yang, G. Li, M. Xiong, F. Liao, and J. Lin, Inorg. Chem. **47**, 2562 (2008).
[12] M. Hase, M. Kohno, H. Kitazawa, N. Tsujii, O. Suzuki, K. Ozawa, G. Kido, M. Imai, and X. Hu, Phys. Rev. B **73**, 104419 (2006).
[13] M. Hase, M. Matsuda, K. Kakurai, K. Ozawa, H. Kitazawa, N. Tsujii, A. Donni, M. Kohno, and X. Hu, Phys. Rev. B **76**, 064431 (2007).
[14] M. Hase, H. Kitazawa, N. Tsujii, K. Ozawa, M. Kohno, and G. Kido, Phys. Rev. B **74**, 024430 (2006).
[15] B. Gu, G. Su, and S. Gao, J. Phys.: Condens. Matter **17**, 6081

(2005).

[16] M. Drillon, M. Belaiche, P. Legoll, J. Aride, A. Boukhari, and A. Moqine, J. Magn. Magn. Mater. **128**, 83 (1993).

[17] Y. Ajiro, T. Asano, K. Nakaya, M. Mekata, K. Ohoyama, Y. Yamaguchi, Y. Koike, Y. Morii, K. Kamishima, H. Aruga-Katori, and T. Goto, in *Proceedings of the International Symposium on Advances in Neutron Scattering Research, Tokai, 2000* [J. Phys. Soc. Jpn. **70** (Suppl. A), 186 (2001)].

[18] A. A. Belik, A. Matsuo, M. Azuma, K. Kindo, and M. Takano, J. Solid State Chem. **178**, 709 (2005).

[19] M. Hase, M. Kohno, H. Kitazawa, O. Suzuki, K. Ozawa, G. Kido, M. Imai, and X. Hu, Phys. Rev. B **72**, 172412 (2005). $Cu_2CdB_2O_6$ exhibits a 1/2 magnetization plateau and AF-LRO. Results of recent studies undertaken by some of the present authors indicate that a spin-1/2 tetramer can account for magnetism of this cuprate.